Enhanced oxidation of aniline using Fe(III)-S(IV) system: Role of different oxysulfur radicals

Yanan Yuan, Tao Luo, Jing Xu, Jinjun Li, Feng Wu, Marcello Brigante, Gilles Mailhot

Enhanced oxidation of aniline using Fe(III)-S(IV) system: Role of different oxysulfur radicals

Yanan Yuan[1,2], Tao Luo[1], Jing Xu[3*], Jinjun Li[1], Feng Wu[1], Marcello Brigante[2], Gilles Mailhot[2]

[1] Department of Environmental Science, School of Resources and Environmental Science, Wuhan University, Wuhan, 430079, China.

[2] Université Clermont Auvergne, CNRS, SIGMA Clermont, Institut de Chimie de Clermont-Ferrand, F-63000 Clermont–Ferrand, France.

[3] State Key Laboratory of Water Resources and Hydropower Engineering Science, Wuhan University, Wuhan 430072, China

Corresponding Authors: Jing Xu (jingxu0506@whu.edu.cn) and Gilles Mailhot (gilles.mailhot@uca.fr)

Abstract

In this paper, the efficiency of Fe(III)-S(IV) system used for advanced oxidation processes (AOPs) has been investigated using aniline as a pollutant model compound in water. The chemical kinetics, influencing factors, and mechanism of aniline oxidation are examined with an emphasis on the contribution of the different oxysulfur radicals (mainly $SO_4^{\bullet-}$ and $SO_5^{\bullet-}$). Our results show a significant enhancement in the efficiency of aniline oxidation observed at pH 4.0 with 1.0 mM S(IV) and 0.1 mM Fe(III) concentrations. Moreover, the degradation efficiency drastically decreases to 10% in the absence of oxygen indicating the significant role of oxygen in this type of process. Through competition kinetic experiments and radical scavenger experiments, it is shown that $SO_5^{\bullet-}$ is responsible for about 60% of the aniline oxidation in the Fe(III)-S(IV) system under the typical conditions investigated in this work. For the first time we have determined the second order rate constant between $SO_5^{\bullet-}$ and aniline ($5.8 \pm 0.6 \times 10^6$ M^{-1} s^{-1} (at pH 3.0) and $SO_4^{\bullet-}$ and aniline $7.7 \pm 0.5 \times 10^9$ M^{-1} s^{-1} (at pH 3.0)). Sequential experiments with successive additions of sulfite drastically improve the oxidation efficiency. These findings may provide a precise understanding of

the overall mechanism and may have promising implications in developing a new cost-effective technology for the treatment of organic compounds-containing water. Furthermore, the results of this work help to understand the relevance and mechanism of organic contaminants oxidation by $SO_5^{\bullet-}$, which has not been given much attention in conventional SR-AOPs using peroxymonosulfate.

Keywords: Aniline, oxidation, sulfite ions, oxysulfur radicals, AOPs.

1. Introduction

Sulfate radical (SR, $SO_4^{\bullet-}$) based advanced oxidation processes (AOPs), namely SR-AOPs, have currently drawn a lot of attention in the field of oxidative decontamination of polluted waters and soils [1-5]. Persulfate (PS, $S_2O_8^{2-}$) and peroxymonosulfate (PMS, HSO_5^-) have been used as $SO_4^{\bullet-}$ precursors in previously reported investigations [6-14] using homogeneous or heterogeneous catalysts containing transition metals such as Fe(II) and Co(II) [15, 16]. Recently, bisulfite (HSO_3^-) has been used to replace PS or PMS in various new transition-metal-catalyzed SR-AOPs systems used for oxidation of several contaminants, such as azo dyes [17-19], phenols, aromatic amines, and arsenite [20-22]. The mechanism of radical chain reactions involving oxysulfur radicals (mainly sulfite radicals ($SO_3^{\bullet-}$), PMS radicals ($SO_5^{\bullet-}$ and $SO_4^{\bullet-}$) during S(IV) autoxidation has been investigated. Generally, $SO_5^{\bullet-}$ is formed from the reaction of $SO_3^{\bullet-}$ with molecular oxygen leading to the formation $SO_4^{\bullet-}$ through further reaction with another $SO_5^{\bullet-}$. However, the involvement of $SO_5^{\bullet-}$ during the oxidation of contaminants has not been completely demonstrated. Neta and Huie reported one-electron redox reactions between $SO_5^{\bullet-}$ and aromatic amines, hydroquinone and other hydroxyphenols [23]. The authors suggested that $SO_5^{\bullet-}$ and not $SO_3^{\bullet-}$ is responsible for the observed degradation of aniline in solution. On the basis of the oxidation potential, $SO_5^{\bullet-}$ can be used to achieve the degradation of organic compounds. Moreover, $SO_5^{\bullet-}$ can accelerate the

Fe(III)/Fe(II) cycle, even if the mechanisms remain unclear. In the absence of oxygen, nearly no oxidation of organic contaminants is observed, which excludes the role played by $SO_3^{\bullet-}$ [20, 21]. Evidence for the Fe(III)/Fe(II) cycle in the presence of a saturated oxygen solution was provided by Brandt et al. [24]. The authors suggested that $SO_5^{\bullet-}$ could be the main oxidant during Fe(II) oxidation into Fe(III). Since the formation of $SO_5^{\bullet-}$ is the main oxygen-consuming step during the overall redox process in the Fe(III)-S(IV) system, the role of oxygen during the regeneration of Fe(III) from Fe(II) has still not been elucidated as well as the enhancement in contaminant oxidation through the activation of iron by S(IV).

In this work, the mechanism of aniline (AN; used as model contaminant) oxidation was investigated in the Fe(III)-S(IV) system with an emphasis on the dual role of oxygen. The changes in the concentrations of Fe(III) and sulfite and the initial pH value of the reaction solution were investigated. The second-order rate constants between AN and $SO_4^{\bullet-}$/$SO_5^{\bullet-}$ were also measured and the contribution made by $SO_4^{\bullet-}$ and $SO_5^{\bullet-}$ evaluated. On the basis of the above results and the experiments performed in this work, the role of oxygen as the oxidant to degrade AN directly and accelerating the cycle between Fe(III) and Fe(II) were analyzed accurately. Furthermore, sequential experiments were also conducted to degrade a high concentration of AN, which provides a facile route for the decontamination of industrial water containing a high concentration of organic compounds. The results of this work will help to understand the relevance and mechanism of organic contaminants oxidation by $SO_5^{\bullet-}$, which has not been given much attention in conventional SR-AOPs using PMS.

2. Materials and methods

2.1. Chemicals

Ferrous sulfate ($FeSO_4 \cdot 7H_2O$, analytical reagent grade), ferric sulfate ($Fe_2(SO_4)_3$), AN, benzotriazole (BTA), N,N-dimethylaniline (DMA), *tert*-butyl alcohol (TBA), ethanol (EtOH),

isopropanol, diphenylamine (DPA), 1,10-phenantroline, NaOH, and H_2SO_4 were purchased from Sinopharm Chemical Reagent Co., Ltd. Sodium sulfite (Na_2SO_3) was purchased from Shanghai Zhanyun Chemical Co., Ltd and its stock solution was prepared just prior to experiments. PMS ($2KHSO_5$. $KHSO_4$. K_2SO_4) and PS ($K_2S_2O_8$) purchased from Sigma-Aldrich served as the compounds providing the strong oxidant, PMS ion (HSO_5^-). Acetonitrile and methanol were HPLC grade and purchased from Fisher Corporation. Na_2CO_3 and $NaHCO_3$ were used to determine the concentration of Na_2SO_3. Ammonium acetate used to prepare the buffer solution for the Fe(II) titration was purchased from Sinopharm Chemical Reagent Co., Ltd. All chemicals were used without any further purification. Ultrapure water with an 18.2 MΩ cm resistivity used in this work was obtained through a water purification system (Liyuan Electric Instrument Co., Beijing, China).

2.2. Experimental setup

Experiments were conducted in a 250 mL open cylindrical reactor held at a constant temperature of 25 °C using circulating thermostatically controlled water through the outer water-jacket of the reaction vessel. Appropriate amounts of the compounds were mixed in the solution and the pH was adjusted upon adding of concentrated NaOH or H_2SO_4 solution using a pHS-3C pH meter (Hinotek, Ningbo, China). The solutions were continuously stirred with a polytetrafluoroethylene-coated magnetic stirrer and each run was started upon the careful addition of the desired volume of the Fe(III) or Fe(II) stock solution. Samples were withdrawn at fixed interval times and analyzed immediately to determine the remaining concentration of AN, S(IV) and Fe(II) in the solution to avoid further reaction. If necessary, predetermined amounts of radical scavengers were added to the solution before AN. In order to investigate the effect of oxygen on the AN degradation, N_2 (99.99%) or pure O_2 (99.99%) were bubbled for 30 min before and throughout the experiment at a constant flow rate of 1 L min^{-1}. A dissolved oxygen meter (8403, AZ Instrument Co. Ltd.) was used to determine the concentration of oxygen in the solution.

2.3. Analytical methods

The disappearance of AN was monitored using high-performance liquid chromatography on a Shimadzu LC-10A system (Kyoto, Japan) equipped with a UV-vis detector (SPD-10AV; Shimadzu) set at 230 nm, a LC-10AT liquid pump, a SIL-10A auto-injector and a ODS-C18 column (25 cm × 4.6 mm, 5μm; Shimadzu, Kyoto, Japan). The eluent was a mixture of acetonitrile/water (v/v, 55/45) at a flow rate of 1.0 mL min^{-1}. The injection volume was 20 μL and the retention time for AN was 4.7 min under these experimental conditions. The concentration of Fe(II) was determined using a colorimetric complexant (1,10-phenanthroline) coupled with spectrophotometric detection at 510 nm using a Shimadzu spectrophotometer UV-1601 [25]. The sulfite concentration was determined by ion chromatography (ICS-90, Dionex, China) using 1 mM $NaHCO_3$ and 8 mM Na_2CO_3 as the eluent and dilute H_2SO_4 as the regenerator. The sample loop size was 50 μL and the eluent flow rate was 1.0 mL min^{-1}.

3. Results and discussion

3.1. AN degradation in Fe(III)/S(IV) system

The AN concentration was monitored in the presence of 0.1 mM of Fe(III) and 1 mM of S(IV) (corresponding to the various ionic forms) at pH 4.0. No significant degradation was determined when Fe(III) and S(IV) were present separately in the solution, while in the presence of both species, AN undergoes significant degradation, revealing its validity in AN degradation. In the first 30 min, about 65% of AN was degraded and a slow degradation rate can be observed up to 80 min (Figure 1). The initial pseudo-first order degradation rate can be estimated to be $1.32 \pm 0.08 \times 10^{-1}$ min^{-1}.

3.1.1 Effect of pH

Modifying the pH from 3 to 7 strongly affects the removal of AN using 0.1 mM of Fe(III) and 1 mM of S(IV), as shown in Figure 2. At pH 7.0, the AN removal was < 10% after 80 min, while

decreasing the pH the degradation efficiency increased, reaching 70% when the initial pH of the solution was 4.0. This effect can be attributed to the stability of the Fe(III)-S(IV) complex as previously reported in different studies [14, 26]. Although it is rather difficult to summarize the overall influence of pH on the Fe(III)-S(IV) induced oxidation (a change in pH can affect the standard reduction potential of the oxidants, the speciation of S(IV) (pKa H_2SO_3/HSO_3^- = 1.8) and stability of Fe(III)), it is interesting to note that at pH 4.0 only HSO_3^- was present in the solution. Under these conditions the formation of a larger amount of the $FeSO_3^+$ complex is expected and is certainly the main raison for the observed higher reactivity. This important result is in agreement with the previously reported studies on cobalt reactivity [27].

3.1.2 The effects of Fe(III)/S(IV) dosage

In order to investigate the effect of the iron and sulfite concentration on the degradation process, the sulfite concentration was varied from 0.6 mM to 1.2 mM using a 0.1 mM of Fe(III) in solution at pH 4.0. Upon increasing the S(IV) concentration from 1 to 1.2 mM, the AN degradation was strongly inhibited with the initial pseudo-first order degradation rate decreased to $8.16 \pm 0.4 \times 10^{-2}$ min^{-1} and the degradation observed after 80 min was ~42%. Increasing the S(IV) concentration inhibits the oxidation of AN through the scavenging reaction between S(IV) and the generated radicals, $SO_4^{\bullet-}$ or $SO_5^{\bullet-}$. Moreover, upon decreasing the S(IV) concentration to 0.6 mM, no significant change in the disappearance of AN was observed at the end of reaction at 80 mins, while a slight increase in the initial reaction rate was observed (Figure 3A). This might due to a co-effect of sulfite dosage and pH change during catalyzing reaction. As discussed in previous work, higher dosage of sulfite lead to a higher generation of H+, while as discussed above, pH lower than 4 would lead to a decrease in AN degradation rate. Nevertheless, low sulfite dosage could not ensure the following reaction (no continuous decrease in AN concentration showed after 5 mins' reaction). Therefore, 1.0 mM of sulfite was used in the following experiments.

A similar trend was observed keeping the S(IV) concentration constant at 1 mM and varying

the Fe(III) concentration from 0.05 to 0.2 mM (Figure 3B). Increasing the Fe(III) concentration may enhance the generation of $SO_3^{\bullet-}$ via intermolecular electron transfer, however, at a high concentration of Fe(III) the formation of colloidal $Fe(OH)_3$ particles, which are responsible for the inhibition of AN degradation, may occur even at pH 4 [21]. Considering these factors, we deemed 0.1/1.0 (mM/mM) as the optimum Fe(III)/S(IV) molar ratio in this system.

3.2. Mechanisms study

Though the mechanisms of Fe(III)/S(IV) on pollutants oxidation has been reported, its role on aniline oxidation are still unclear, especially the contribution of the different oxysulfur radicals (mainly $SO_4^{\bullet-}$ and $SO_5^{\bullet-}$) and the role of dissolved oxygen on Fe(III)/S(IV) system. These unsolved questions were hence investigated, by determining the reactivity constants between AN and oxysulfur free radicals, and studying the effect of oxygen on each parameters.

3.2.1 Determination of the reactivity constants with $SO_4^{\bullet-}$ and $SO_5^{\bullet-}$

Prior to the determination of the contribution of oxysulfur radicals by quenching experiments, the second-order rate constants between AN and $SO_4^{\bullet-}$ ($k_{AN,SO_4^{\bullet-}}$) or $SO_5^{\bullet-}$ ($k_{AN,SO_5^{\bullet-}}$) were determined using chemical competition kinetic experiments with radical scavengers, as listed in Table 1. The bimolecular reactivity constant with $SO_4^{\bullet-}$ was determined using a conventional Fe(II)-PS system in which $SO_4^{\bullet-}$ and $OH^{\bullet}$ were generated at an initial pH of 3. This pH was selected to avoid the natural oxidation of Fe(II) into Fe(III) with dissolved oxygen. Isopropanol (2-PrOH) was used to scavenge $HO^{\bullet}$ [39] while BTA was employed as a chemical competitor for the reaction with $SO_4^{\bullet-}$ (R1 and R2).

$$AN + SO_4^{\bullet-} \rightarrow products_1 \qquad k_{AN,SO_4^{\bullet-}} \qquad \text{(R1)}$$

$$BTA + SO_4^{\bullet-} \rightarrow products_2 \qquad k_{BTA,SO_4^{\bullet-}} = 3.5\times10^9 M^{-1}s^{-1} \qquad \text{(R2)}$$

Considering the first-order decay of chemical species and applying the competition kinetic method, the relationship between the decay of the two species is given by Eq. 1:

$$\ln\left(\frac{[AN]_0}{[AN]_t}\right) = \frac{k_{AN,SO_4^{\bullet-}}}{k_{BTA,SO_4^{\bullet-}}} \times \ln\left(\frac{[BTA]_0}{[BTA]_t}\right) \qquad \text{(Eq. 1)}$$

Where $[AN]_0$ and $[BTA]_0$, and $[AN]_t$ and $[BTA]_t$ are initial concentrations and concentrations at time *t* of AN and BTA, respectively. The slope of the linear fit of the experimental data of $\ln\left(\frac{[BTA]_0}{[BTA]_t}\right)$ *vs* $\ln\left(\frac{[AN]_0}{[AN]_t}\right)$ gives the ratio of two second order rate constants $\frac{k_{AN,SO_4^{\bullet-}}}{k_{BTA,SO_4^{\bullet-}}}$. In Figure 4 the linear fit gives a slope of 2.20 ±0.13, which corresponds to $k_{AN,SO_4^{\bullet-}}$ = 7.7 ±0.5 × 10^9 $M^{-1}s^{-1}$.

For the determination of the second order rate constant between AN and $SO_5^{\bullet-}$ ($k_{AN,SO_5^{\bullet-}}$), DMA was selected to be the competition reagent for AN to react with $SO_5^{\bullet-}$ in the Fe(III)-S(IV) system. EtOH, which has a negligible reactivity with $SO_5^{\bullet-}$ (< 1 × 10^3 M^{-1} s^{-1}) was used to selectively scavenge any other radicals, such as $HO^{\bullet}$ and $SO_4^{\bullet-}$ ($k_{EtOH,HO^{\bullet}}$ = 1.9 × 10^9 M^{-1} s^{-1} and $k_{EtOH,SO_4^{\bullet-}}$ = 7.7 × 10^7 M^{-1} s^{-1}). A concentration of 0.5 M of EtOH was used in the solution during the experiments. The same approach was adopted for sulfate radical used in this system and $k_{AN,SO_5^{\bullet-}}$ was found to 5.8 ±0.6 × 10^6 M^{-1} s^{-1}.

3.2.2 Roles of $SO_4^{\bullet-}$ and $SO_5^{\bullet-}$

Although the formation of $SO_4^{\bullet-}$ and $SO_5^{\bullet-}$ in this system is demonstrated, their relative contributions to the oxidation of AN are still needed to be investigated. Under the adopted experimental conditions, hydroxyl radicals cannot be generated in the system in a sufficient concentration for the oxidation of organic contaminants mainly due to the high concentration of S(IV) and acidic environment [24, 28]. The fact that no significant inhibition of AN degradation was observed using different TBA concentrations (Figure. S1) suggests that $HO^{\bullet}$ are not generated in the reaction system. The initial degradation rate of AN (R_{AN}^{d}) was calculated under a specific concentration of the scavenger, when the concentration of TBA was 100 times higher than that of

AN, the corresponding contribution of $HO^{\bullet}$ was < 3% (Table 2), which validate this hypothesis.

Then, to dissociate the contribution of $SO_4^{\bullet-}$ and $SO_5^{\bullet-}$, the different scavengers were added into the reaction system. Scavenging $SO_3^{\bullet-}$ by EtOH even at a very high concentration (0.5 M) can be neglected due to the very high reactivity between $SO_3^{\bullet-}$ and dissolved oxygen ($k_{O_2,SO_3^{\bullet-}}$ = 1.5 × 10^9 M^{-1} s^{-1} [29]). However, EtOH can be used to differentiate between $SO_4^{\bullet-}$ and $SO_5^{\bullet-}$ due to the large difference (> 10^4-fold) between the $k_{EtOH,SO_4^{\bullet-}}$ and $k_{EtOH,SO_5^{\bullet-}}$ values [34-36].

In order to set the appropriate EtOH concentration to scavenge $SO_4^{\bullet-}$ only without interfering with the $SO_5^{\bullet-}$ reactivity with AN, experiments using different concentrations of EtOH (in the range of 5 to 500 × 10^2 [AN]) were performed (Figure 5A). As expected, the AN degradation presents a slight decrease upon increasing the EtOH concentration, due to the scavenging effect of EtOH on the $SO_5^{\bullet-}$ reactivity at a high EtOH/AN ratio. In the absence and presence of the inhibitor (EtOH), we can assume that the initial $SO_4^{\bullet-}$ radical yield is the same in both solutions and the standard competition kinetic equations (Eq. 2–3) can be used to estimate the inhibition efficiency (ρ) of EtOH on AN oxidation. In these equations, $k'_{EtOH=0}$ and k'_{EtOH} represent the pseudo-first-order rate constants of AN reacting with $SO_4^{\bullet-}$ in the absence and presence of various concentrations of EtOH, respectively.

$$\frac{k'_{EtOH=0}}{k'_{EtOH}} - 1 = \frac{k_{SO_4^{\bullet-},EtOH}}{k_{SO_4^{\bullet-},AN}} \times \frac{[EtOH]_0}{[AN]_0} \qquad \text{(Eq. 2)}$$

which, after rearrangement gives:

$$\frac{k'_{EtOH}}{k'_{EtOH=0}} = \frac{1}{\frac{k_{SO_4^{\bullet-},EtOH}}{k_{SO_4^{\bullet-},AN}} \times \frac{[EtOH]_0}{[AN]_0} + 1} \qquad \text{(Eq. 3)}$$

The inhibition efficiency of [EtOH] (ρ) on AN oxidation by $SO_4^{\bullet-}$ can be determined as:

$$\rho(\%) = 1 - \frac{k'_{EtOH}}{k'_{EtOH=0}} \times 100 \qquad \text{(Eq. 4)}$$

$$\rho(\%) = \left(1 - \frac{1}{\frac{k_{SO_4^{\bullet-},EtOH}}{k_{SO_4^{\bullet-},AN}} \times \frac{[EtOH]_0}{[AN]_0} + 1} \right) \qquad \text{(Eq. 5)}$$

Equation 5 can be plotted as $y = 1 - \frac{1}{ax+1} \times 100$ with $a = \frac{k_{SO_4^{\bullet-},EtOH}}{k_{SO_4^{\bullet-},AN}} = 7.7 \times 10^7 / 7.7 \times 10^9 = 0.01$.

In Figure 5B, the inhibition efficiency is reported as a function of $[EtOH]_0/[AN]_0$ and the inhibition efficiency can reach ~98%, which reasonably shows that the complete inhibition of $SO_4^{\bullet-}$ was achieved. However, the model fit overestimates the inhibition efficiency. This effect was attributed to the fact that the presence of $SO_5^{\bullet-}$ was not considered in the equations.

DPA and EtOH were also used in order to discriminate between the contribution of $SO_4^{\bullet-}$ and $SO_5^{\bullet-}$ to the degradation of AN in the Fe(III)-S(IV) system. In the presence of 50 μM of DPA, which is able to quantitatively trap both $SO_4^{\bullet-}$ and $SO_5^{\bullet-}$ [28], almost no degradation of AN was observed in solution, as reported in Figure. 6, indicating that $SO_4^{\bullet-}$ and $SO_5^{\bullet-}$ are the most important reactive species generated in the solution. Using 50 mM of EtOH, which is able to scavenge $SO_4^{\bullet-}$ and not significantly $SO_5^{\bullet-}$, the AN degradation was inhibited by ~50%. The contribution of these two radicals was then determined and, as shown in Table 2, the inhibition efficiency attributed to $SO_4^{\bullet-}$ was only 35.9 ±1.0% and it is possible to determine the contribution from $SO_5^{\bullet-}$ to the degradation of AN was ~60%.

3.2.3 Effect of dissolved oxygen

To shed light onto the effect of oxygen on the oxidation of AN, different experiments were performed at different oxygen concentrations in the solution upon continuous bubbling pure O_2, air and N_2 throughout the whole experiment. As depicted in Figure S2, when the experiments were conducted in the presence of air or pure O_2 ($[O_2]$ > 20 mg L^{-1} in the solution) bubbling, a plateau corresponding to 70% AN degradation was found after 20-30 min. However, the efficiency

decreases to 10% in the nitrogen purged solutions. This result implies that oxygen plays an important role in the transformation of AN in the Fe(III)-S(IV) system. On the other hand, there were no remarkable differences among the degradation effects between bubbling of pure O_2 or air after 80 min of reaction, which illustrates that air purging supply enough dissolved oxygen during the whole reaction.

Experiments were also conducted to investigate the consumption of S(IV); the generation of Fe(II); the oxygen concentration and pH variation during the whole reaction under oxic (pure O_2 and air bubbling) or anoxic conditions (N_2 bubbling). Referring to the consumption of S(IV), the sulfite ions are oxidized to S(VI) very quickly especially in an oxygen saturated solution (Figure 7A) due to the formation of $SO_3^{\bullet-}$ (equilibria 1 and 2 in Table S1). Oxic conditions accelerated the formation of $FeSO_3^+$ by the cyclic of iron species [14, 30]. Figure 7B showed the formation of Fe(II) during the oxidation of AN. Obvious generation of Fe(II) was observed in the absence of oxygen (rapidly increase up to 36.6 μM after 5 min), while its generated amount was much less in the aerated and O_2 saturated solutions, that only a slight formation of Fe(II) was observed after the first 2 min followed by its disappearance due to its fast oxidation into Fe(III). Figure. 7C confirmed the oxygen consumption during the reaction (decreased sharply in the first 10 min before reaching a stable concentration of 8 mg L^{-1} by re-oxygenation), which might due to the combined contribution of Fe(II) oxidation and $SO_5^{\bullet-}$ generation (Table S1). The pH change also showed differences at different atmosphere conditions (Figure 7D). As have been discussed in previous work, H^+ is mainly generated through the reaction of $SO_4^{\bullet-}$ and HSO_3^- (reaction 9-10 in Table S1). In saturated oxygen solutions, the larger decrease in pH indicated the acceleration of the oxysulfur radical cycle and the subsequent enhancement in the Fe(III)-S(IV) cycle. Overall, offering excessive oxygen favors of the cyclic of Fe(III)/Fe(II) and the generation of $SO_5^{\bullet-}$ by $SO_3^{\bullet-}$ oxidation, which both contributed to the AN degradation. In the meantime, higher generated amount of oxysulfur free radicals also accelerate the acidification of solution during reaction.

3.3. Investigation of the catalytic cycle

Sequential experiments were conducted with a fixed concentration of Fe(III) (0.1 mmol.L^{-1}) and multiple additions of SO_3^{2-} at pH 4.0 in order to check the effect of SO_3^{2-} on catalytic degradation of a highly concentrated solution of AN. In this experiment, the concentration of AN was 100 µM and 1.0 mM S(IV) was added to the solution at the beginning and then 1.0 mM S(IV) was added to the reaction mixture every 20 min, The results are displayed in Figure 8 and indicate that multiple additions of sulfite can nearly completely degrade the AN after 140 min of reaction (> 90% degradation efficiency). However, it is important to mention that the high concentration of S(IV) did not improve the degradation of AN. In fact, when 7 mM S(IV) was added to the solution in one portion, the reaction was strongly inhibited. An increase in the S(IV) dosage was not always able to enhance the oxidation of the organic contaminants. On the contrary, an excessively high S(IV) concentration retards the subsequent reaction, as observed in Figure 3A and in the literature [17, 31]. This result is in agreement with the previously reported studies on high [M(n)]/[S(IV)] and low [S(IV)]/[O_2] ratios (M(n): heavy-metal ion) [32, 33]. Otherwise, the system tends to be less oxidative due to the competition between target pollutants and oxysulfur free radicals and the anoxic conditions. As the source for generating oxysulfur radicals, an appropriate concentration of S(IV) can increase the oxidation reaction.

4. Conclusions

This work shows that high efficiency in AN decontamination can be achieved in the Fe(III)-S(IV) system under specific conditions. Consequently, oxysulfur radicals including $SO_4^{\bullet-}$ and $SO_5^{\bullet-}$ are the dominant oxidants, which are mainly responsible for the degradation of AN. Furthermore, $SO_5^{\bullet-}$ also played a relatively important role in the oxidation of AN. Its contribution is considerable (~60%) when compared to all the radical species involved in the oxidation process. In addition, the

rate constants $k_{AN,SO_4^{\bullet-}}$ and $k_{AN,SO_5^{\bullet-}}$ were estimated to be 7.7 ± 0.5 × 10^9 $M^{-1}s^{-1}$ and 5.8 ± 0.6 × 10^6 M^{-1} s^{-1}, respectively. The experiments conducted with different levels of oxygen in the solution showed that dissolved oxygen plays a significant role in generating the radicals involved in the oxidation process. This work, not only provides a feasible candidate for use in the efficient oxidation of aromatic amines, but also highlights the novel concept that the role of $SO_5^{\bullet-}$ cannot be neglected in future studies.

Acknowledgements

This work was supported by the National Natural Science Foundation of China (NSFC-CNRS_ PRC No. 21711530144 and CNRS No. 270437). This work was also supported by the "Federation des Recherches en Environnement" through the CPER "Environnement" founded by the "Région Auvergne," the French government and FEDER from European community. The authors gratefully acknowledge the financial support from the China Scholarship Council provided to Yanan Yuan to study at the University Clermont Auvergne in Clermont-Ferrand, France. The comments from the anonymous reviewers are also appreciated.

References

[1] M. Ahmad, A.L. Teel, R.J. Watts, Mechanism of persulfate activation by phenols, Environ. Sci. Technol. 47 (2013) 5864-5871.

[2] G.P. Anipsitakis, D.D. Dionysiou, Degradation of organic contaminants in water with sulfate radicals generated by the conjunction of peroxymonosulfate with cobalt, Environ. Sci. Technol. 37 (2003) 4790-4797.

[3] G.P. Anipsitakis, T.P. Tufano, D.D. Dionysiou, Chemical and microbial decontamination of pool water using activated potassium peroxymonosulfate, Water Res. 42 (2008) 2899-2910.

[4] A. Ghauch, A.M. Tuqan, N. Kibbi, Naproxen abatement by thermally activated persulfate in aqueous systems, Chem. Eng. J. 279 (2015) 861-873.

[5] T. Zeng, X. Zhang, S. Wang, H. Niu, Y. Cai, Spatial confinement of a Co_3O_4 catalyst in hollow metal-organic frameworks as a nanoreactor for improved degradation of organic pollutants， Environ. Sci. Technol. 49 (2015) 2350-2357.

[6] G.P. Anipsitakis, D.D. Dionysiou, M.A. Gonzalez, Cobalt-mediated activation of peroxymonosulfate and sulfate radical attack on phenolic compounds. implications of chloride ions，Environ. Sci. Technol. 40 (2006) 1000-1007.

[7] Y. Feng, D. Wu, Y. Deng, T. Zhang, K. Shih, Sulfate radical-mediated degradation of sulfadiazine by $CuFeO_2$ rhombohedral crystal-catalyzed peroxymonosulfate: synergistic effects and mechanisms, Environ. Sci. Technol. 50 (2016) 3119-3127.

[8] H. Guo, N. Gao, Y. Yang, Y. Zhang, Kinetics and transformation pathways on oxidation of fluoroquinolones with thermally activated persulfate, Chem. Eng. J. 292 (2016) 82-91.

[9] C. Liang, H.W. Su, Identification of sulfate and hydroxyl radicals in thermally activated persulfate, Ind. Eng. Chem. Res. 48 (2009) 472-475.

[10] L.W. Matzek, K.E. Carter, Activated persulfate for organic chemical degradation: A review, Chemosphere. 151 (2016) 178-188.

[11] C. Qi, X. Liu, J. Ma, C. Lin, X. Li, H. Zhang, Activation of peroxymonosulfate by base: Implications for the degradation of organic pollutants, Chemosphere. 151 (2016) 280-288.

[12] B.T. Zhang, Y. Zhang, Y. Teng, M. Fan, Sulfate radical and its application in decontamination technologies, Crit. Rev. Env. Sci. Tec. 45 (2015) 1756-1800.

[13] T. Zhang, H. Zhu, J.-P. Croué, Production of sulfate radical from peroxymonosulfate induced by a magnetically separable $CuFe_2O_4$ spine l in water: efficiency, stability, and mechanism, Environ. Sci. Technol. 47 (2013) 2784-2791.

[14] Y. Wu, R. Prulho, M. Brigante. W. Dong, K. Hanna, G. Mailhot, Activation of persulfate by Fe(III) species: Implications for 4-tert-butylphenol degradation, J. Hazard. Mater. 322 (2017) 380-386.

[15] E.M. Contreras, stoichiometry of sulfite oxidation by oxygen during the determination of the volumetric mass transfer coefficient, Ind. Eng. Chem. Res. 47 (2008) 9709-9714.

[16] P. Hu, M. Long, Cobalt-catalyzed sulfate radical-based advanced oxidation: A review on heterogeneous catalysts and applications, Appl. Catal., B. 181 (2016) 103-117.

[17] L. Chen, X. Peng, J. Liu, J. Li, F. Wu, Decolorization of orange II in aqueous solution by an Fe(II)/sulfite system: replacement of persulfate, Ind. Eng. Chem. Res. 51 (2012) 13632-13638.

[18] W. Shi, Q. Cheng, P. Zhang, Y. Ding, H. Dong, L. Duan, X. Li, A. Xu, Catalytic decolorization of methyl orange by the rectorite–sulfite system, Catal. Commun. 56 (2014) 32-35.

[19] D. Zhou, L. Chen, C. Zhang, Y. Yu, L. Zhang, F. Wu, A novel photochemical system of ferrous sulfite complex: Kinetics and mechanisms of rapid decolorization of Acid Orange 7 in aqueous solutions, Water Res. 57 (2014) 87-95.

[20] Y. Yuan, S. Yang, D. Zhou, F. Wu, A simple Cr(VI)–S(IV)–O_2 system for rapid and simultaneous reduction of Cr(VI) and oxidative degradation of organic pollutants, J. Hazard. Mater. 307 (2016) 294-301.

[21] J. Xu, W. Ding, F. Wu, G. Mailhot, D. Zhou, K. Hanna, Rapid catalytic oxidation of arsenite to arsenate in an iron(III)/sulfite system under visible light, Appl. Catal., B. 186 (2016) 56-61.

[22] D.N. Zhou, L. Chen, J.J. Li, F. Wu, Transition metal catalyzed sulfite auto-oxidation systems for oxidative decontamination in waters: A state-of-the-art minireview, Chem. Eng. J. 346 (2018) 726-738.

[23] R.E. Huie, P. Neta, One-electron redox reactions in aqueous solutions of sulfite with hydroquinone and other hydroxyphenols, J. Phys. Chem. 89 (1985) 3918-3921.

[24] C. Brandt, I. Fabian, R. Van Eldik, Kinetics and mechanism of the iron(III)-catalyzed autoxidation of sulfur(IV) oxides in aqueous solution. Evidence for the redox cycling of iron in the presence of oxygen and modeling of the overall reaction mechanism, Inorg. Chem. 33 (1994) 687-701.

[25] H. Tamura, K. Goto, T. Yotsuyanagi, M. Nagayama, Spectrophotometric determination of iron(II) with 1,10-phenanthroline in the presence of large amounts of iron(III), Talanta. 21 (1974) 314-318.

[26] Y.J. Lee, G.T. Rochelle, Oxidative degradation of organic acid conjugated with sulfite oxidation in flue gas desulfurization: products, kinetics, and mechanism, Environ. Sci. Technol. 21 (1987) 266-272.

[27] Y. Yuan, D. Zhao, J. Li, F. Wu, M. Brigante, G. Mailhot, Rapid oxidation of paracetamol by cobalt(II) catalyzed sulfite at alkaline pH, Catal. Today. 323 (2018) 155-160.

[28] D. Zhou, Y. Yuan, S. Yang, H. Gao, L. Chen, Roles of oxysulfur radicals in the oxidation of acid orange 7 in the Fe(III)/sulfite system, J. Sulfur Chem. 36 (2015) 373-384.

[29] R.E. Huie, P. Neta, Chemical behavior of $SO_3^{\bullet-}$ and $SO_5^{\bullet-}$ radicals in aqueous solutions, J. Phys. Chem. 88 (1984) 5665-5669.

[30] I. Grgićc, M. Pozničc, M. Bizjak, S(IV) Autoxidation in atmospheric liquid water: The role of Fe(II) and the effect of oxalate, J. Atmos. Chem. 33 (1999) 89-102.

[31] L. Zhang, L. Chen, M. Xiao, L. Zhang, F. Wu, L. Ge, Enhanced decolorization of orange II solutions by the Fe(II)–sulfite system under xenon lamp irradiation, Ind. Eng. Chem. Res. 52 (2013) 10089-10094.

[32] L.B. Carvalho, M.V. Alipazaga, W.C.T. Crivelente, N. Coichev, The autoxidation of Co(II)/2-Aamino-2-Hydroxymethyl-1,3-Propanediol in the pesence of Mn(II) and S(IV), Bioinorg. React. Mech. 5 (2004) 101-108.

[33] D.T.F. Kuo, D.W. Kirk, C.Q. Jia, The chemistry of aqueous S(IV)-Fe-O_2 system: state of the art, J. Sulfur Chem. 27 (2006) 461-530.

[34] L. Dogliotti, E. Hayon, Flash photolysis of per[oxydi]sulfate ions in aqueous solutions. The sulfate and ozonide radical anions, J. Phys. Chem. 71 (1967) 2511-2516.

[35] C.L. Clifton, R.E. Huie, Rate constants for hydrogen abstraction reactions of the sulfate radical, $SO_4^{\bullet-}$. Alcohols, Int. J. Chem. Kinet. 21 (1989) 677-687.

[36] E. Hayon, A. Treinin, J. Wilf, Electronic spectra, photochemistry, and autoxidation mechanism of the sulfite-bisulfite-pyrosulfite systems. $SO_2^{\bullet-}$, $SO_3^{\bullet-}$, $SO_4^{\bullet-}$, and $SO_5^{\bullet-}$ radicals, J. Am. Chem. Soc. 94 (1972) 47-57.

[37] G.V. Buxton, C.L. Greenstock, W.P. Helman, A.B. Ross, Critical review of rate constants for reactions of hydrated electrons chemical kinetic data base for combustion chemistry. Part 3: Propane, J. Phys. Chem. Ref. Data 17 (1988) 513-886.

[38] D.B. Naik, P.N. Moorthy, Studies on the transient species formed in the pulse radiolysis of benzotriazole, Radiat. Phys. Chem. 46 (1995) 353-357.

[39] P. Neta, R.E. Huie, One-electron redox reactions involving sulfite ions and aromatic amines, J. Phys. Chem. 89 (1985) 1783-1787.

Table 1. A summary of the second-order rate constants k of the reactions of the chemical scavengers with the oxysulfur radicals.

Reaction	Rate constant, k ($M^{-1} s^{-1}$)	Reference
EtOH + $SO_4^{\bullet-}$	7.7×10^7	[34, 35]
EtOH + $SO_3^{\bullet-}$	$< 2 \times 10^3$	[36]
EtOH + $SO_5^{\bullet-}$	$< 1 \times 10^3$	[36]
EtOH + $HO^{\bullet}$	1.9×10^9	[37]
Benzotriazole + $SO_4^{\bullet-}$	3.5×10^9	[38]
$(C_6H_5)_2NH$ + $SO_3^{\bullet-}$	$<1.0 \times 10^7$ (pH 3-7)	[39]
$(C_6H_5)_2NH$ + $SO_5^{\bullet-}$	5×10^7 (pH 3)	[39]
$C_6H_5NH_2$ + $SO_3^{\bullet-}$	$<1.0 \times 10^6$ (pH 13)	[39]
$C_6H_5NH_2$ + $SO_5^{\bullet-}$	$\sim 3 \times 10^6$ (pH 13)	[39]
	$5.8 \pm 0.6 \times 10^6$	this work
$C_6H_5NH_2$ + $SO_4^{\bullet-}$	$7.7 \pm 0.5 \times 10^9$	this work
tert-Butyl alcohol + $HO^{\bullet}$	7.6×10^8	[17]
tert-Butyl alcohol + $SO_4^{\bullet-}$	9.1×10^5	[17]
2-PrOH+ $HO^{\bullet}$	1.6×10^9	[39]
2-PrOH+ $SO_4^{\bullet-}$	4.7×10^6	[39]

Table 2. The initial degradation rate of AN (R_{AN}^{d}) in the Fe(III)-S(IV) system in the presence of various radical scavengers.

Parameter	**No scavenger**	**$[TBA]_0/[AN]_0 = 100$**	**$[EtOH]_0/[AN]_0 = 5000$**	**$[DPA]_0/[AN]_0 = 100$**
R_{AN}^{d} (μM min^{-1})	0.513 ± 0.015	0.500 ± 0.025	0.316 ± 0.005	0.008 ± 0.004
Contribution of radicals	$(1 - R_{DPA}/R) \times 100 = 98.4 \pm 0.8$ %			
Contribution of $HO^{\bullet}$	$(1 - R_{TBA}/R) \times 100 = 2.5 \pm 4.9$ %			
Contribution of $SO_4^{\bullet}$	$(1 - R_{EtOH}/R) \times 100 - 2.5\% = 35.9 \pm 1.0$ %			
Contribution of $SO_5^{\bullet}$	98.4% – 38.4% = 60.0%			

Figures Captions

Fig. 1: Degradation of AN (10 μM) in the presence of sulfites (1 mM) and Fe(III) (0.1 mM) at pH = 4.0 in aerated solution.

Fig. 2: Degradation of AN (10 μM) using Fe(III) (0.1 mM) and S(IV) (1 mM) at different pH values in aerated solution.

Fig. 3: Degradation of AN (10 μM) using different Fe(III)/S(IV) ratios at pH = 4.0 in aerated solution; A) $[Fe(III)]_0$ = 0.1 mM, B) $[S(IV)]_0$ = 1.0 mM.

Fig. 4: Linear fit of ln([AN]0/[AN]t) vs ln([BTA]0/[BTA]t) in the Fe(II)-$S_2O_8^{2-}$ system conducted in the dark at pH 3.0. The dashed lines denote the 95% confidence of the linear fit. The initial concentrations are: $[AN]_0$ = [BTA] = 10 μM, [Isopropanol] = 2.0 mM, $[Fe(II)]_0$ = 0.5 mM and $[K_2S_2O_8]$ = 5.0 mM.

Fig. 5: (A) Degradation of AN with time using different $[EtOH]_0/[AN]_0$ ratios. (B) Inhibition efficiency (ρ) as a function of the $[EtOH]_0/[AN]_0$ ratio. Conditions: $[AN]_0$ = 10 μM, $[Fe(III)]_0$ = 0.1 mM, $[S(IV)]_0$ = 1.0 mM and pH = 4.0.

Fig. 6. AN degradation in the Fe(III)-S(IV) system in the absence (no scavengers) and presence of different radical scavengers. Conditions: $[AN]_0$ = 10 μM, $[Fe(III)]_0$ = 0.1 mM, $[S(IV)]_0$ = 1.0 mM and pH = 4.0.

Fig. 7: Variation in S(IV) (A), Fe(II) (B), $[O_2]$ (C) and pH (D) during the oxidation of AN in the Fe(III)-S(IV) system. Conditions: $[AN]_0$ = 10 μM, $[Fe(III)]_0$ = 0.1 mM, $[S(IV)]_0$ = 1.0 mM and pH = 4.0.

Fig. 8: Degradation of AN (100 µM) during in the Fe(III)-S(IV) upon the sequential addition of S(IV) every 20 min under oxygen and air bubbling at pH 4.0. Conditions: $[Fe(III)]_0$ = 0.1 mM and $[S(IV)]_0$ = 1.0 mM.

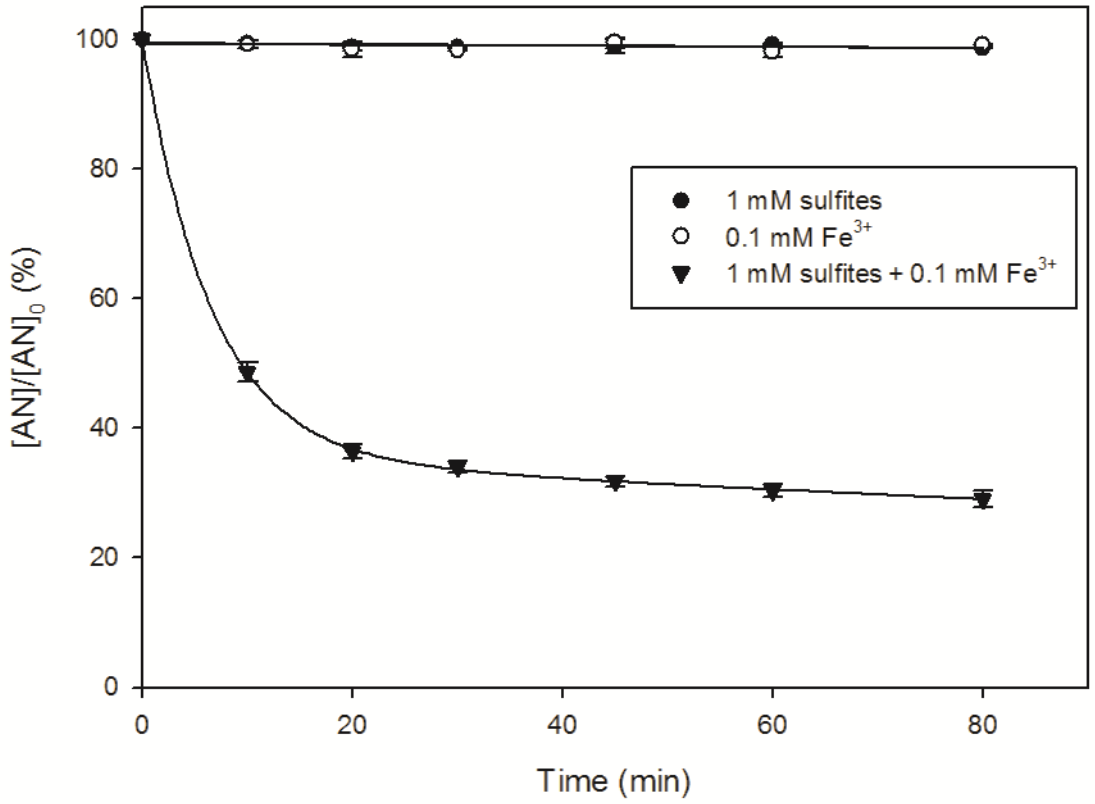
100
80
60
40
20
0
0
20
40
60
80
[AN]/[AN]0 (%)
Time (min)
1 mM sulfites
0.1 mM Fe3+
1 mM sulfites + 0.1 mM Fe3+

Fig. 1

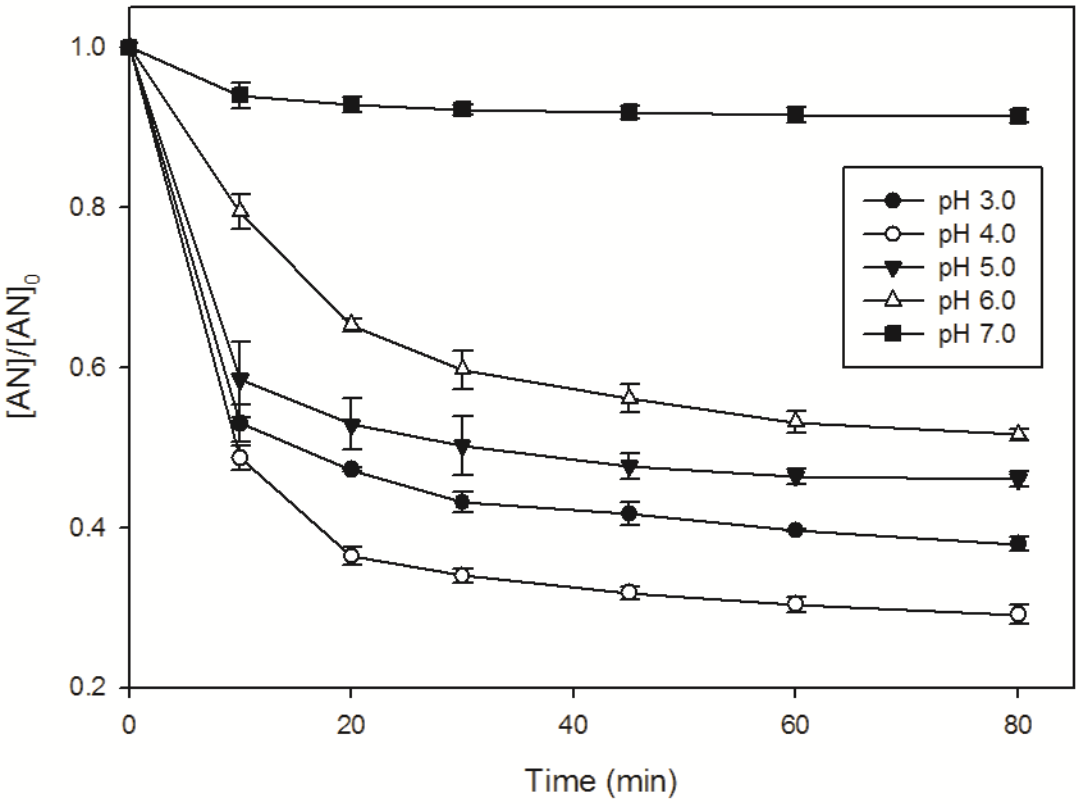
1.0
0.8
0.6
0.4
0.2
[AN]/[AN]0
0
20
40
60
80
Time (min)
pH 3.0
pH 4.0
pH 5.0
pH 6.0
pH 7.0

Fig. 2

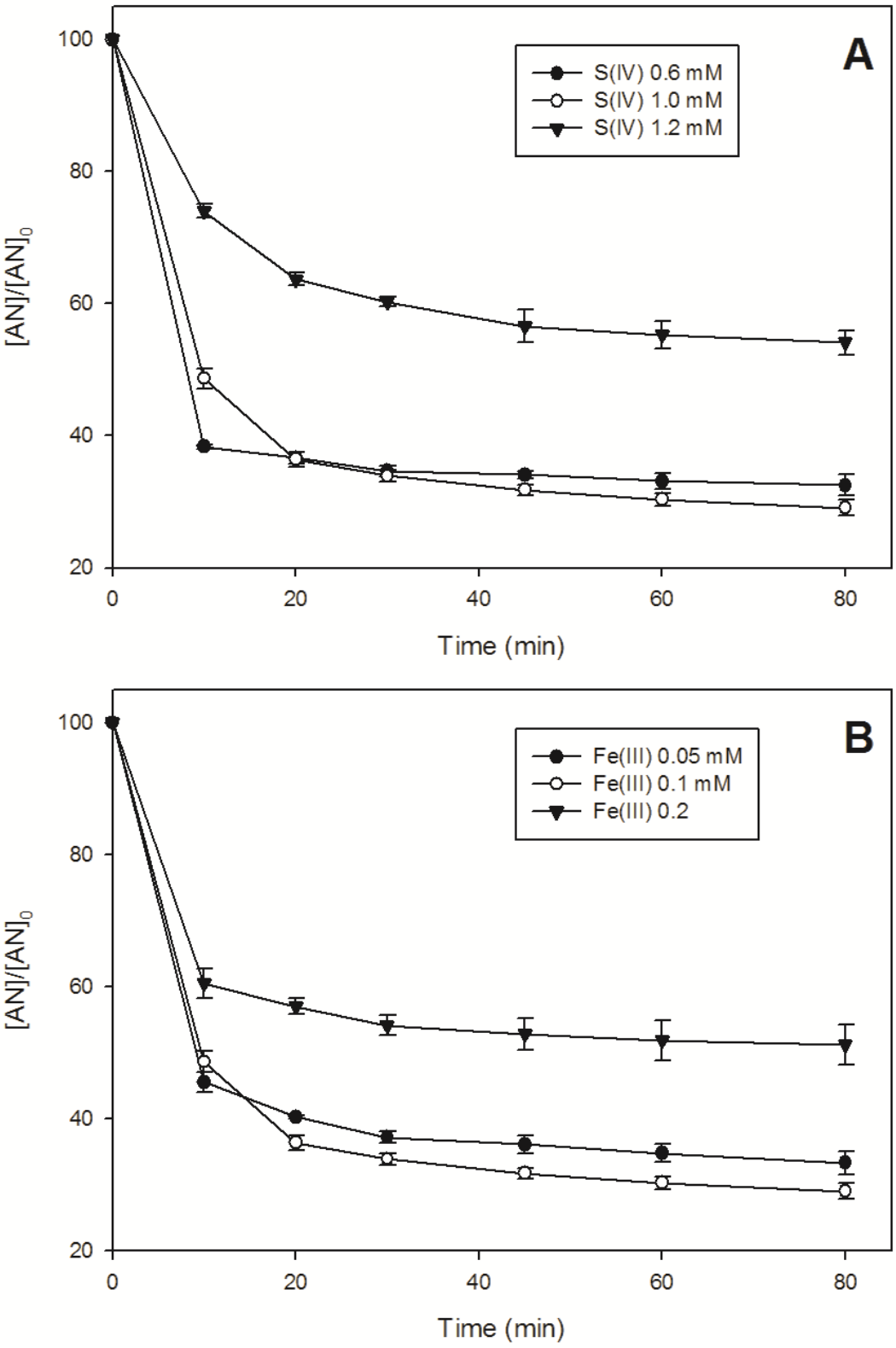
A
S(IV) 0.6 mM
S(IV) 1.0 mM
S(IV) 1.2 mM
[AN]/[AN]0
Time (min)
B
Fe(III) 0.05 mM
Fe(III) 0.1 mM
Fe(III) 0.2
[AN]/[AN]0
Time (min)

Fig. 3

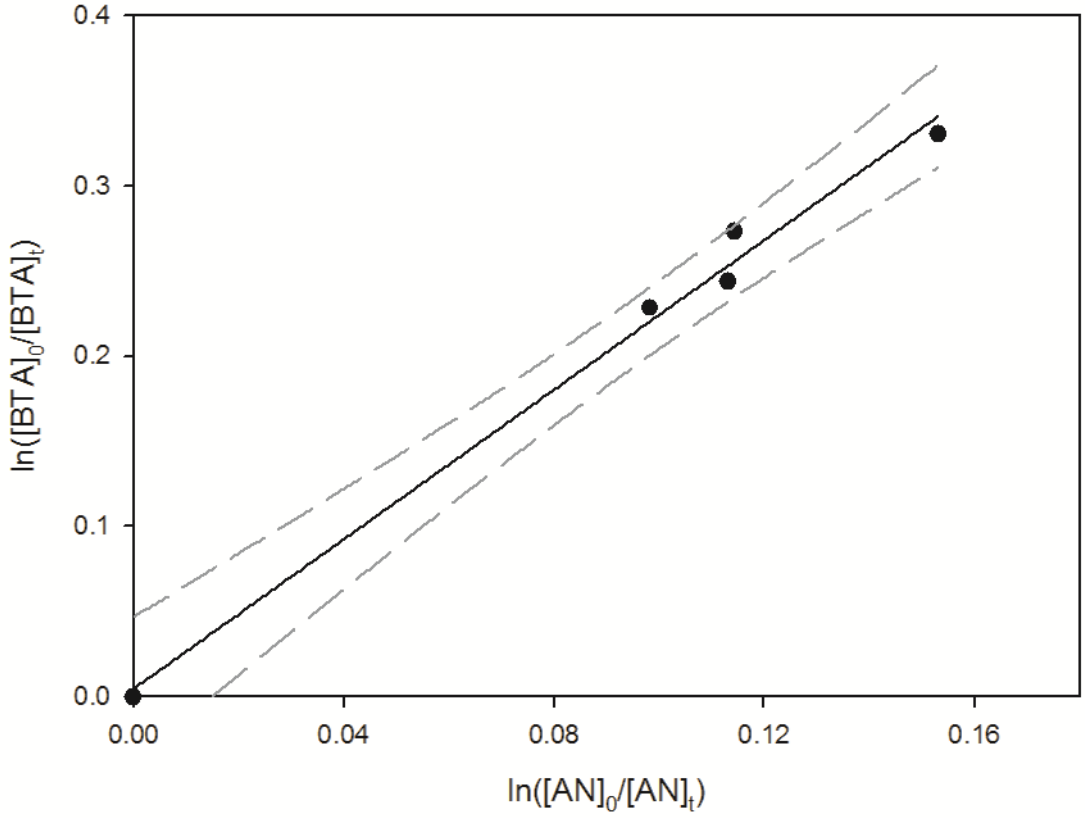

Fig. 4

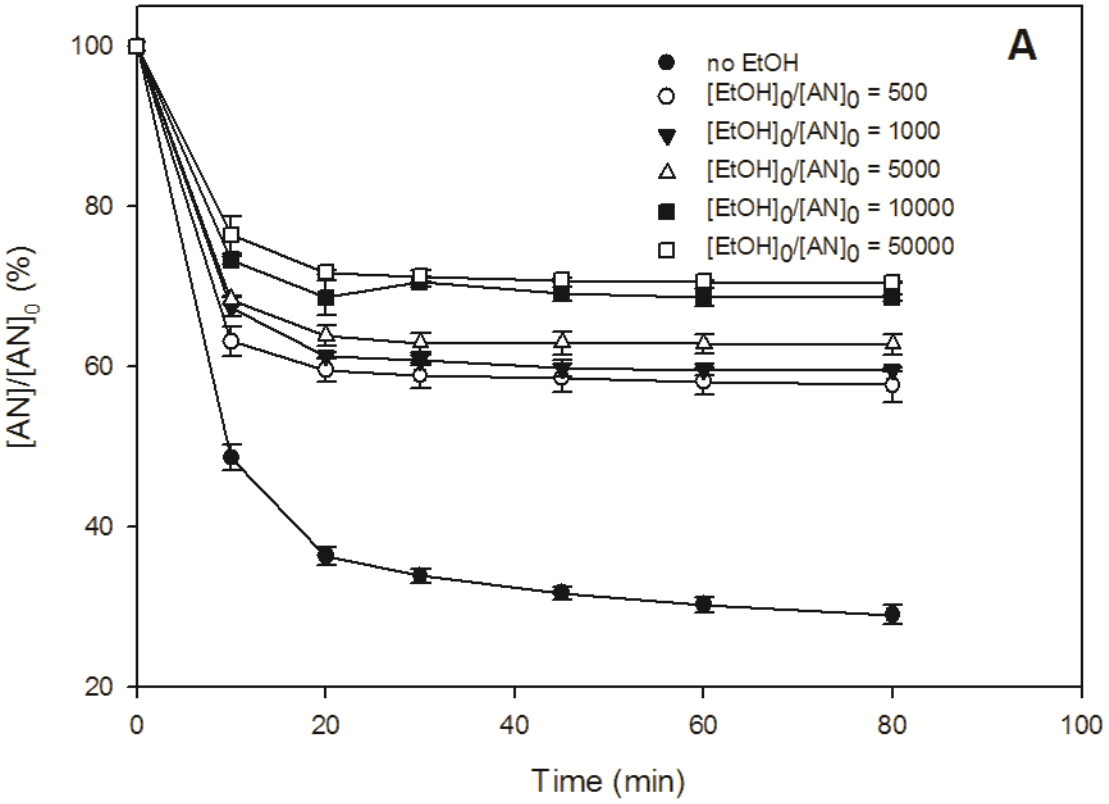
A
no EtOH
[EtOH]0/[AN]0 = 500
[EtOH]0/[AN]0 = 1000
[EtOH]0/[AN]0 = 5000
[EtOH]0/[AN]0 = 10000
[EtOH]0/[AN]0 = 50000
[AN]/[AN]0 (%)
Time (min)
100
80
60
40
20
0
20
40
60
80
100

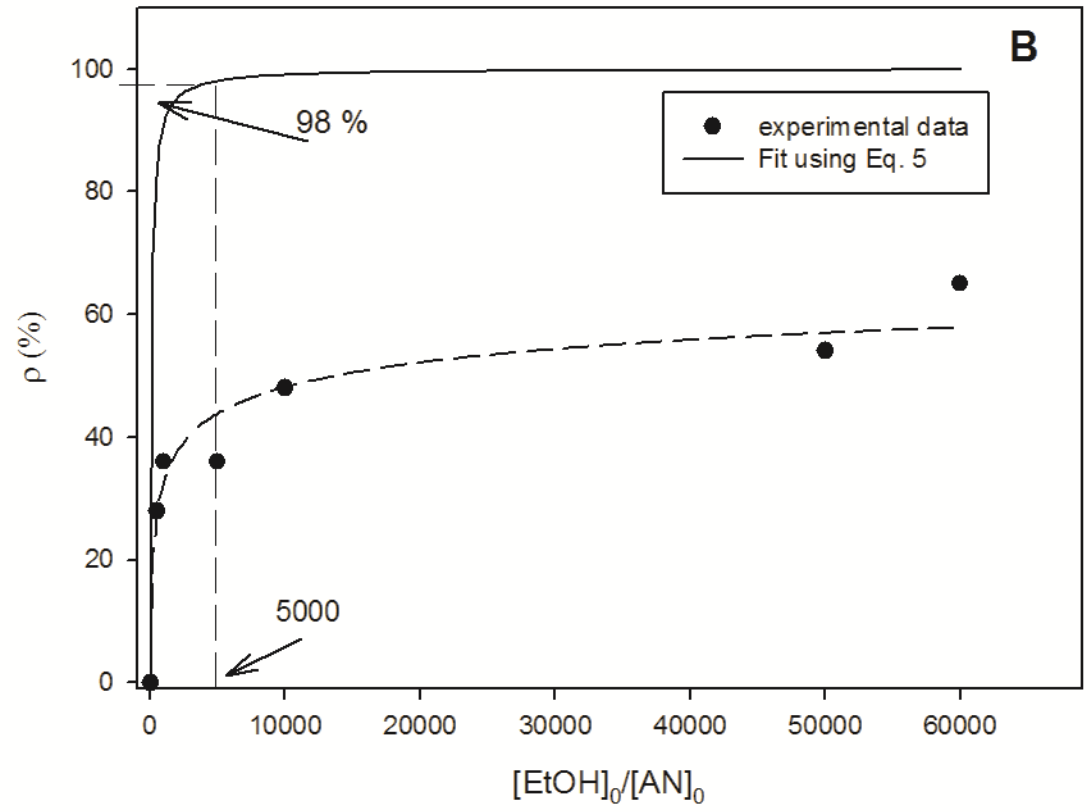
B
experimental data
Fit using Eq. 5
98 %
5000
ρ (%)
[EtOH]0/[AN]0
100
80
60
40
20
0
0
10000
20000
30000
40000
50000
60000

Fig. 5

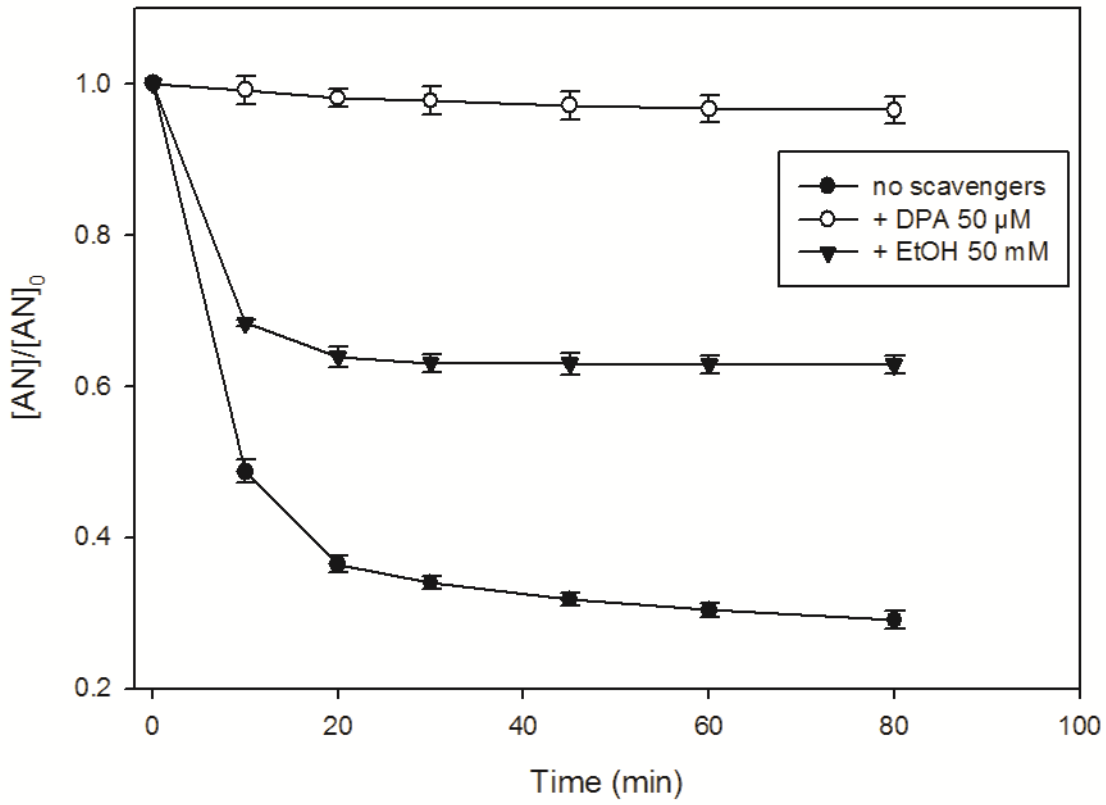
1.0
0.8
0.6
0.4
0.2
[AN]/[AN]0
0
20
40
60
80
100
Time (min)
no scavengers
+ DPA 50 µM
+ EtOH 50 mM

Fig. 6

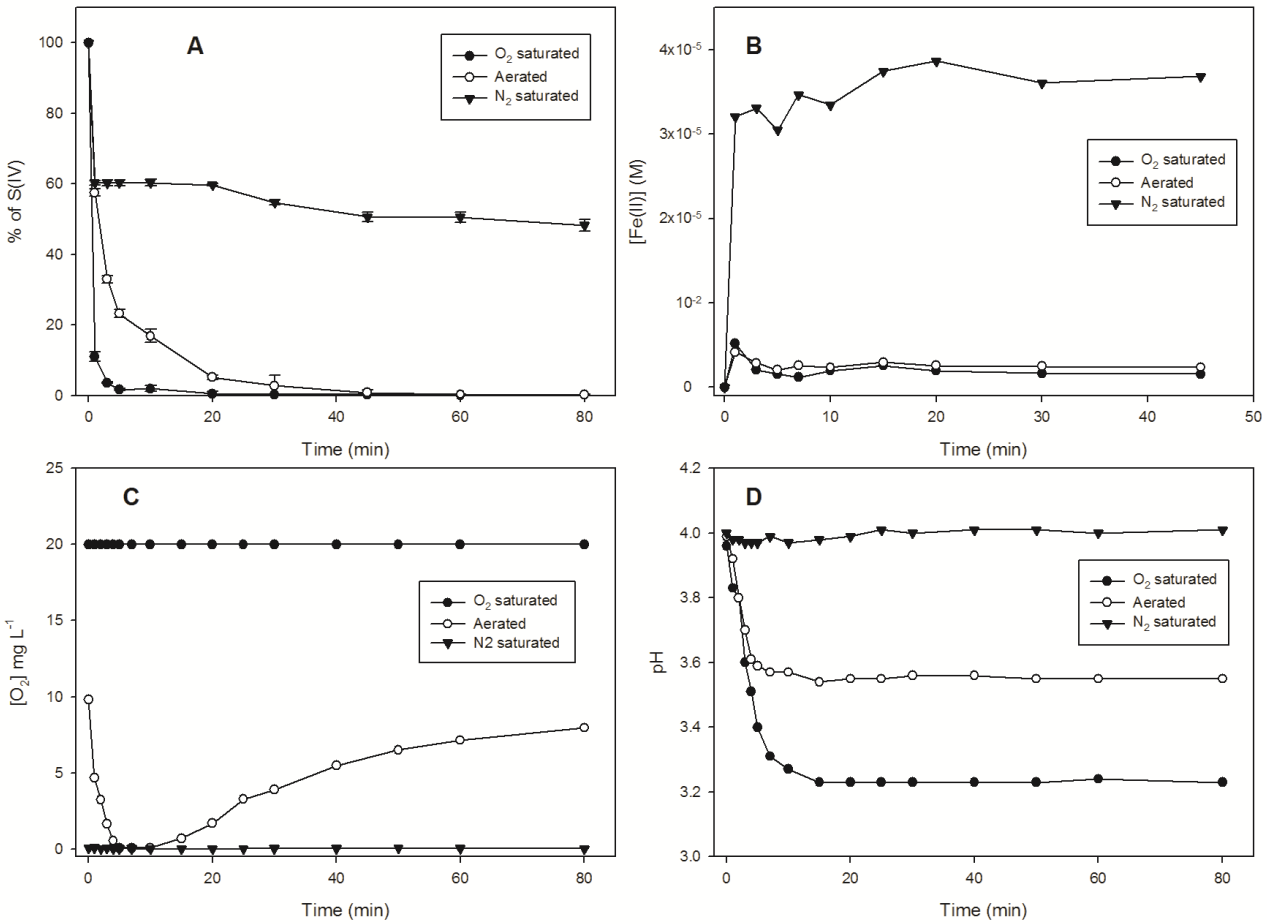
A
% of S(IV)
Time (min)
O2 saturated
Aerated
N2 saturated
B
[Fe(II)] (M)
Time (min)
O2 saturated
Aerated
N2 saturated
C
[O2] mg L-1
Time (min)
O2 saturated
Aerated
N2 saturated
D
pH
Time (min)
O2 saturated
Aerated
N2 saturated

Fig. 7

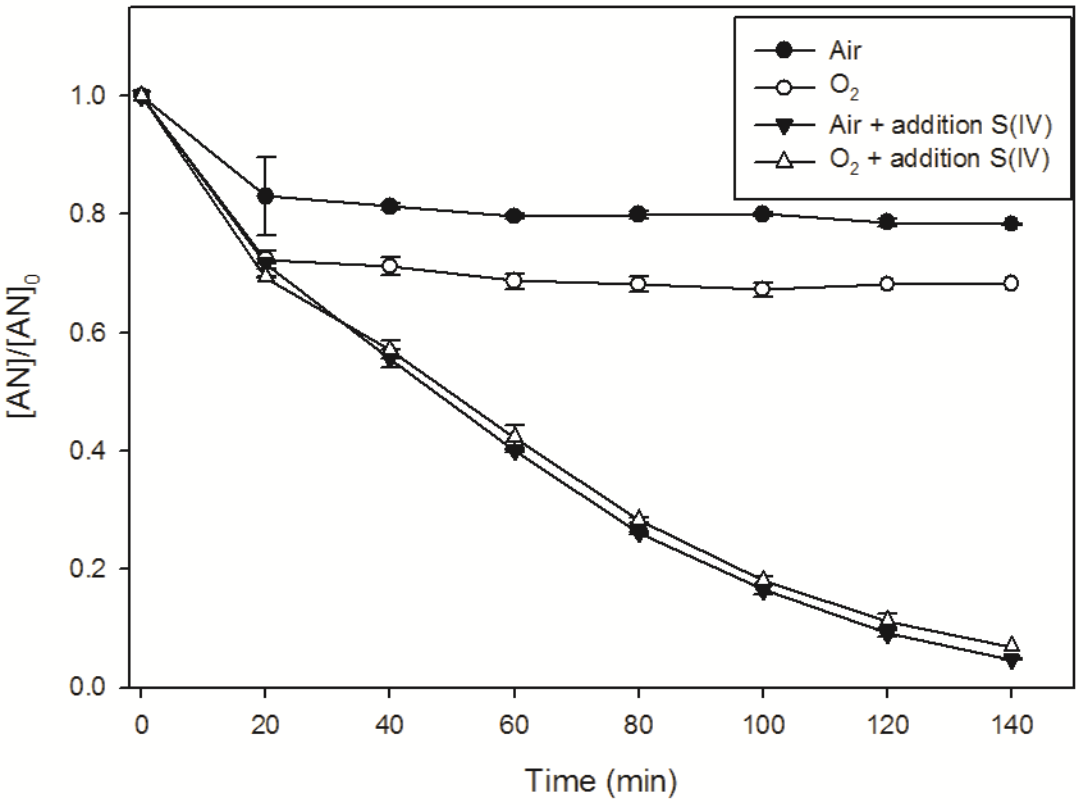
Air
O2
Air + addition S(IV)
O2 + addition S(IV)
[AN]/[AN]0
1.0
0.8
0.6
0.4
0.2
0.0
0
20
40
60
80
100
120
140
Time (min)

Fig. 8